

Synthesis and optical properties of organic semiconductor: zirconia nanocomposites

M. Sagmeister · U. Brossmann · E. J. W. List ·
R. Ochs · D. V. Szabó · R. Saf · W. Grogger ·
E. Tchernychova · R. Würschum

Abstract Oxide nanoparticles were used as carrier for organic semiconductor materials. Stable suspensions of ZrO₂ nanoparticles coated with anthracene, pentacene, or para-hexaphenyl were obtained by microwave plasma synthesis of ZrO₂ cores, subsequent in situ coating with organic compounds, and in situ dispersion in ethylene glycol. Powders of coated oxide nanoparticles were synthesized for comparison. The successful coating and a small uniform size distribution of the ZrO₂ cores were confirmed by comprehensive characterization including photoluminescence, absorption spectroscopy, electron microscopy,

electron energy loss spectroscopy, mass spectrometry, and X-ray diffraction. Powder compacts of anthracene-coated ZrO₂ particles showed good air stability and a significant blue shift accompanied by an attenuation of the emission lines at higher vibronic orders in comparison to samples of pure anthracene as received. For para-hexaphenyl-coated nanoparticles, the same photoluminescence characteristics are observed as for pure para-hexaphenyl. In the case of pentacene-coated nanoparticles indication for degradation is found.

Keywords Nanocrystalline oxides · Micro wave plasma synthesis · Organic semiconductors · Photoluminescence · Transmission electron microscopy · Electron energy loss spectroscopy · Core-shell nanoparticles

M. Sagmeister · U. Brossmann (✉) · R. Würschum
Institute of Materials Physics, Graz University
of Technology, Petersgasse 16, 8010 Graz, Austria
e mail: brossmann@tugraz.at

E. J. W. List
Institute of Solid State Physics, Graz University
of Technology, Petersgasse 16, 8010 Graz, Austria

R. Ochs · D. V. Szabó
Institute for Materials Research III, Karlsruhe Institute
of Technology, 76021 Karlsruhe, Germany

R. Saf
Institute of Chemistry and Technology of Organic
Materials, Graz University of Technology,
Stremayergasse 16, 8010 Graz, Austria

W. Grogger · E. Tchernychova
Institute for Electron Microscopy, Graz University
of Technology, Steyrergasse 17, 8010 Graz, Austria

Introduction

Nano-scaled core shell materials made of a metal oxide core covered with a functional organic or oxide shell offer great potentials for obtaining novel and improved properties, e.g., as electronic, luminescent, or sensor materials (Vollath 2008). Nanoparticles with organic shells may also open new processing routes for device fabrication, such as liquid phase processing of the practically insoluble organic semiconductors pentacene and para-hexaphenyl (p-6P). Initial studies in this direction were conducted on

anthracene-coated oxide nanoparticles with an additional protective layer of poly methyl-methacrylate (PMMA) showing a significant change of the optical properties with respect to the pure organic constituents (Vollath and Szabó 2006).

The present article reports on an in-depth study of the synthesis and the optical properties on *in situ* dispersed oxide nanoparticles coated with organic semiconducting materials. In addition to anthracene, pentacene and para-hexaphenyl were studied due to their technological importance. Pentacene is one of the most prominent organic semiconductors (Anthony 2007). Both organic field effect transistors (OFETs) and sensor devices based on pentacene films have been successfully demonstrated and are subject of intense ongoing research (Dimitrakopoulos and Malenfant 2002; Zhu et al. 2002). Para-hexaphenyl has a high application potential as luminescent material in optoelectronic devices due to its highly efficient blue emission (Era et al. 1995). Using optical down conversion to obtain green and red light emission, p-6P-based multicolour or white organic light emitting devices (OLEDs) can be fabricated (Tasch et al. 1997).

One drawback for a large scale application of both pentacene and para-hexaphenyl is the negligible solubility in common solvents at ambient conditions. Pentacene, for instance, has to be either heated (Minakata and Natsume 2005) or synthesized through a soluble precursor (Brown et al. 1996) for liquid processing, such as ink-jet printing (Böberl et al. 2007). The present study therefore investigates an alternative approach to make pentacene and p-6P suitable for liquid processing, namely microwave plasma synthesis and *in situ* dispersion of organic-coated oxide nanoparticles. Our previous studies have shown that these nanocomposite particles form stable dispersions in ethylene glycol (Sagmeister et al. 2008).

In difference to hot wall reactors, microwave plasma synthesis is particularly suitable for producing organic inorganic composite nanoparticles due to its low processing temperatures compatible with organic materials. Additionally, an electrostatic charging of the particles originating in the plasma process in combination with residence time in the plasma of only a few milliseconds leads to a uniform, small size of the oxide cores, since grain growth and agglomeration of

the core particles prior to coating is suppressed (Vollath and Szabó 1999, 2006).

Besides a comprehensive characterization by electron microscopy, mass spectroscopy, and X-ray diffraction, the present study focuses on the study of the optical properties of these composite nanomaterials. Optical spectroscopy techniques, particularly in measurements of the absorption and photoluminescence (PL), represent powerful tools for investigating the structure of the π -conjugated organic molecule coatings and their interaction with the oxide cores and solvents (Gundlach et al. 1999; Nijegorodov et al. 1997; Lakowicz 2006). Photoluminescence spectroscopy is highly sensitive with respect to the electronic and vibrational structure. In the case of organic semiconductors based on π -conjugated organic molecules, information about the surroundings of the molecules and their interaction with each other can be deduced by the peak positions and the intensity ratios of the different vibronic states in the recorded spectra. In solid state luminescence, generally a red shift in comparison with gas phase spectra and in case of crystalline phases the so-called Davydov splitting is observed (Kamura et al. 1974). Additional information on the energy transfer and relaxation processes and thus the local environment of the pentacene molecules may be obtained by comparing PL and absorption spectra, as these processes occur on different timescales (Lakowicz 2006). Therefore, the combination of optical spectroscopy methods is expected to provide comprehensive information on the structure of the pentacene and p-6P coatings and the agglomeration of the particles, as well as the role of solvents and in particular traces of impurities which may quench optical emission lines.

Experimental

Chemical vapor synthesis of the oxide nanoparticles (cores) is performed in a microwave plasma. Details of the synthesis method in general are described in (Vollath and Szabó 2006; Vollath 2008). In the reaction zone, the precursors are decomposed and the nanocrystalline (n -)ZrO₂ cores are formed. The non-agglomerated core particles are subsequently coated in a second step. Collection of the particles has either been accomplished by passing the gas stream through

a washing bottle filled with ethylene glycol (liquid dispersions) or by deposition on a cooled finger (powder samples). Figure 1 shows schematically the experimental setup with liquid dispersion powder collection.

Following our previous studies (Sagmeister et al. 2008; Broßmann et al. 2007), the liquid metal organic precursor Zr(IV)-n-butoxide was used for synthesizing the n-ZrO₂ core particles. Pure anthracene, pentacene, or para-hexaphenyl vapor from a second evaporation source was used for organic coating. In a typical run, 2 ml of metal organic precursor with a feeding rate of 5–8 ml/h and 150 mg of the organic coating material were used. In the case of powder samples, about 200–300 mg of product could be harvested. A pulsed microwave plasma (2.45 GHz, on/off period: 1 ms/1 ms) with an effective power of 150 to 300 W was applied at a gas pressure of about 10 mbar. This allowed both to achieve a quantitative formation of small, uniform oxide cores and to maintain relatively low temperatures in the coating zone in the range of 200–250 °C (pentacene, anthracene) or 380–420 °C (p-6P) to reduce degradation of the organic coating material.

Reference samples of anthracene and pentacene dispersed in ethylene glycol without n-ZrO₂ cores were prepared in the same experimental setup. In this case, however, only the evaporation source for the polyacenes was used without any microwave plasma. Before characterization by optical measurements, all in situ dispersed samples (Table 1) have been ultrasonicated for 15 min. Alternatively, dry powder samples of coated particles were obtained by collecting the nanoparticles on a water-cooled finger and scraping them off with a razor blade. For photoluminescence and x-ray diffraction (XRD) studies, the

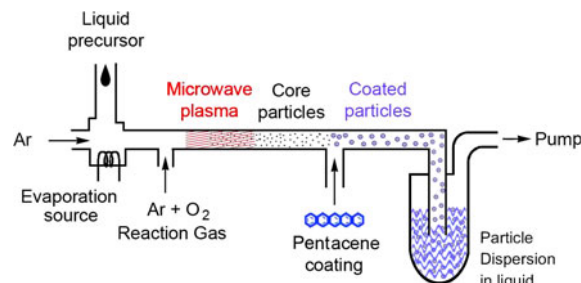


Fig. 1 Schematic drawing of the microwave plasma synthesis of ZrO₂ nanoparticles, in situ coating with organic materials (e.g., pentacene), and in situ dispersion in ethylene glycol

powders were pressed into small pellets using a uniaxial pressure of 1 GPa. Reference samples of pure powder compacts were made by pressing pellets of as received anthracene and pentacene. Table 1 gives an overview of the samples used in this study.

Transmission electron microscopy (TEM) was done with microscopes of Tecnai F20 series at 200 kV. Electron energy loss spectroscopy (EELS) measurements on organic semiconductor-coated n-ZrO₂ were performed with a Gatan Multiscan CCD/EELS, operating at 200 keV. The acquisition of EEL-spectra was performed in TEM image mode, using a 2-mm spectrometer entrance aperture and a dispersion of 0.3 eV/channel. The samples for TEM and EELS measurements were taken by dipping lacey carbon films on 300 mesh copper grids into the collected powder. This preparation method has the advantage of being free of organic solvents, combined with the slight disadvantage of getting agglomerates instead of isolated powder particles. As many parts of the agglomerates are located across the holes of the support film, EELS analysis without any influence of the support film is assured. Additionally, uncoated n-ZrO₂ nanoparticles were re-dispersed in isopropanol and collected on polymer coated Cu grid for TEM studies.

The photoluminescence measurements were carried out using a computer-controlled Shimadzu RF-5301 PC spectrofluorophotometer with a Xe-arc lamp as light source in the case of anthracene and pentacene (see Lakowicz 2006), for a general description. For the PL measurements of the p-6P-coated samples, a Horiba-Jobin-Yvon Fluorolog3 spectrofluorophotometer was used. An excitation wavelength of 350 nm was used, which is below the onset of strong absorption in the ZrO₂ cores. The PL spectra were recorded for wavelengths in the range from about 370 to 600 nm, taking about 1 min for a full scan. The dispersions have been diluted to the point where no significant self absorption could be observed. For better comparability all PL spectra have been normalized to each other. The PL and absorbance could not be quantitatively assessed as the particle content obtained by in situ dispersion and resulting optical density could only be roughly estimated based on the yield for dry powders under identical synthesis conditions.

Optical absorption was measured using a Varian Cary 50 UV VIS spectrophotometer. The absorbance of pure ethylene glycol in the measuring cuvette as a

Table 1 Preparation conditions of the samples investigated

Composition	Preparation route	Sample number #
ZrO ₂	Powder	0
Anthracene	As received (powder)	1
ZrO ₂ /anthracene core shell	In situ dispersed	2
Pentacene	Powder	3
ZrO ₂ /pentacene core shell	In situ dispersed	4
Para hexa phenyl	As received (powder)	5
ZrO ₂ /para hexa phenyl core shell	In situ dispersed	6
	Powder	7
	In situ dispersed	8
	In situ dispersed and aged	9
	As received (powder)	10
	Powder	11
	In situ dispersed	12

reference was scanned first and then automatically subtracted from all following measurements.

Mass spectrometry was performed on a Micromass ToFSpec 2E Time-of-Flight mass spectrometer, an instrument designed for matrix-assisted laser desorption/ionisation (MALDI). The instrument is equipped with a nitrogen laser (337 nm wavelength, operated at a frequency of 5 Hz) and a time lag focusing unit. Ions were generated by irradiation just above the threshold laser power. Spectra were recorded in reflectron mode applying an accelerating voltage of 20 kV and externally calibrated with a suitable mixture of poly(ethyleneglycol)s (PEG). The spectra of 100–150 shots were averaged. Analysis of data was done with MassLynx-Software V3.5 (Micromass/Waters, Manchester, UK). It is important to note that the solid samples were deposited directly on the target without addition of a matrix material to avoid any contaminations or interferences. Consequently, the mass spectra discussed below are standard laser desorption/ionisation (LDI) spectra.

Results and discussion

Stable suspensions of pentacene and para-hexaphenyl-coated nanoparticles were successfully prepared using the in situ dispersion technique described above. A particle content in the order of 1 g/L was estimated from the amount of powder collected on a cold finger under similar processing conditions. The particles stayed dispersed for several weeks and no

sedimentation was observed under ambient conditions (Sagmeister et al. 2008).

Transmission electron microscopy was used to characterize the morphology and the size of the particles. Micrographs recorded on both re-dispersed uncoated n-ZrO₂ (Fig. 2, left) and, exemplarily for organic semiconductor-coated nanoparticles, on p-6P-coated n-ZrO₂ (Fig. 2b, right) show a small mean grain size ($d < 5$ nm) and a narrow particle size distribution. The TEM measurements also show that both the uncoated and p-6P-coated nanoparticles form small agglomerates with a size in the order of 50 nm, as previously observed in dynamic light scattering (DLS) measurements (Sagmeister et al. 2008).

Electron-energy loss spectroscopy shows clear evidence of organic coating on n-ZrO₂ particles. Figure 3a shows exemplarily zero loss EELS spectra recorded on the p-6P-coated particles as well as on uncoated n-ZrO₂ and on an amorphous carbon film as reference samples. For uncoated n-ZrO₂ and the pure carbon film, the EELS spectra at low energy losses (Fig. 3a) are in good agreement with literature data from the EELS-atlas (Ahn and Krivanek 1983). The characteristic loss peaks at 13 and 22 eV are ascribed to volume plasmons in Zr and C. The EELS spectra of p-6P-coated n-ZrO₂ particles show both contributions thus indicating an organic coating.

The assumption of a p-6P coating on the n-ZrO₂ cores is also supported by EELS data for higher loss energies giving a clear indication for the presence of an organic coating. Figure 3b shows the background corrected core loss spectra of uncoated n-ZrO₂ (#0) as

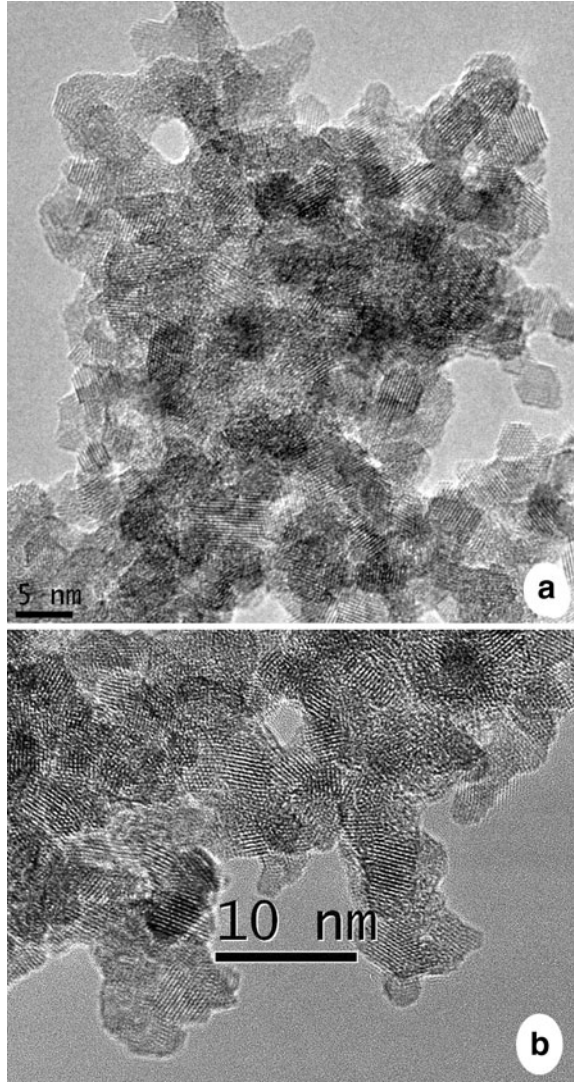


Fig. 2 TEM micrograph of uncoated n-ZrO₂ (**a**) and para hexaphenyl coated n-ZrO₂ (**b**)

a reference and of p-6P-coated particles (#11). The reference n-ZrO₂ is more or less free of C, whereas clear indications of C=C bonding (π^*) at an energy loss of 285 eV, of C H bonding (σ^*) at an energy loss of around 293 eV, and of C C bonding (σ^*) at an energy loss around 299 eV are present in the p-6P-coated material (Gordon et al. 2003). Zr M2 and Zr M3 major edges are found in both spectra. Due to the precautions taken during analysis, a C-signal stemming from the lacey carbon film can be excluded.

In contrast to the EELS-studies, high-resolution TEM micrographs (Fig. 2b) of the p-6P-coated ZrO₂-

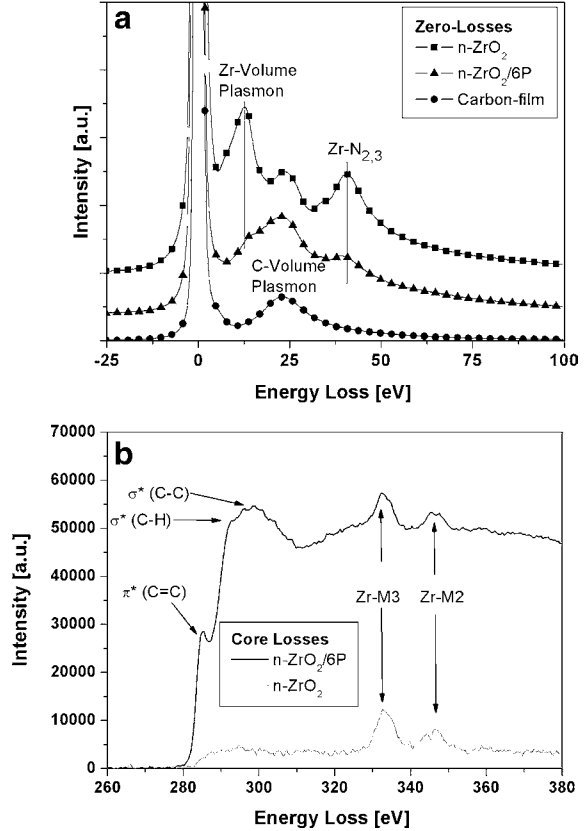


Fig. 3 Electron energy loss spectra of the low loss region (**a**) for uncoated and para hexaphenyl coated n-ZrO₂ and amorphous carbon. Part (**b**) shows the core loss region of uncoated and p-6P coated ZrO₂ nanoparticles

nanoparticles (#11) do not show clear evidence for coating, because the individual particles are not clearly separated. This may at least indicate that the p-6P molecule with a length of 2.6 nm is not attached perpendicular to the length axis on the surface of the nanoparticles, otherwise it would act as a spacer and separated nanoparticles should be observed. In the case of a monolayer coating parallel to the length axis of the p-6P molecule, the height of the molecule is below the resolution of the TEM.

Anthracene-coated nanoparticles

For initial studies of the optical properties of polyacene-coated nanoparticles, the material system n-ZrO₂-anthracene was chosen. The photoluminescence of anthracene as received and anthracene-coated particles were probed both on powder samples

pressed into tablet-shaped pellets (# 1 and 3) and on in situ processed dispersions in ethylene glycol (# 2 and # 4). In the case of consolidated powder samples, the PL spectra of anthracene-coated n-ZrO₂ and pure anthracene significantly differ from each other. Compared to pure anthracene compacts (# 1, Fig. 4a) and literature data (Vollath and Szabó 2006; Nijegorodov et al. 1997; Gordon et al. 2003; Lumb 1978), a blue shift and an increase in relative intensity of the emission at 408 nm and an attenuation of the emission lines at longer wavelengths occurs in anthracene-coated n-ZrO₂ (# 3). These variations are probably due to interactions of the coating with the core material. Qualitatively very similar results have been reported for HfO₂/anthracene/PMMA nanocomposite particles (Vollath and Szabó 2006) although the peak positions there are shifted to longer wavelengths by 10–15 nm. This can be ascribed to the different core material (HfO₂) and the additional PMMA coating.

In contrast to the powder samples, both as-received anthracene and the anthracene-coated ZrO₂ particles dispersed in ethylene glycol (# 2 and # 4) appear identical after ultrasonication (Fig. 4b). This indicates that the anthracene coating may have dissolved in ethylene glycol, as it is attached to the oxide cores only by weak van-der-Waals bonds. This view is supported by literature data according to which anthracene is soluble in ethylene glycol (although only to minor extend) (Sizmann 1959). Another indication for the dissolving of anthracene from the ZrO₂ cores is the fact that the initially milky suspensions formed by in situ dispersion of coated particles (# 4) became almost clear after ultrasonication. Based on the differences in the solid state spectra (Fig. 4a), we can conclude, that it was possible to coat the particles successfully. On the other hand, the identical spectra of the dispersed coated particles and of the as received anthracene dispersion infer that the organic material has not been degraded during the synthesis or subsequent storage in ambient conditions.

Pentacene-coated nanoparticles

For pentacene-coated nanoparticles, both absorption and luminescence were studied. Absorption spectra were recorded on pentacene-coated ZrO₂-nanoparticles and on pure pentacene reference samples which

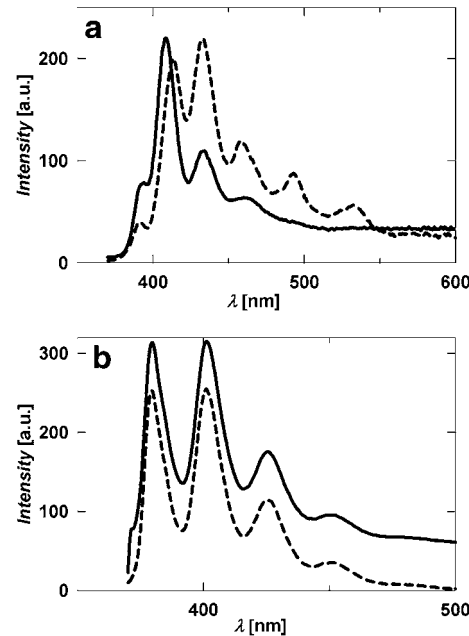


Fig. 4 PL spectra of anthracene coated ZrO₂ nanoparticles (solid line) and of pure anthracene (dashed line) as pressed pellets (**a**, samples #1, #3) and dispersed in ethylene glycol (**b**, samples #2, #4)

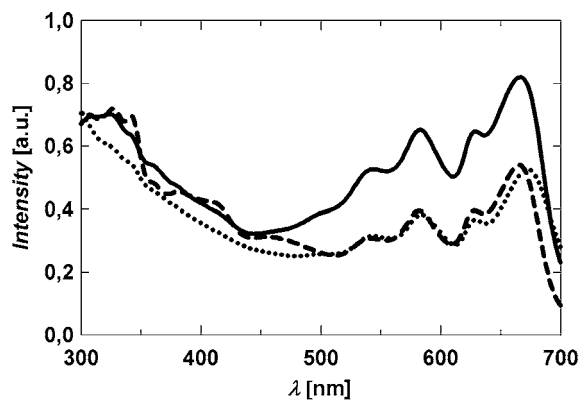


Fig. 5 Absorption spectra of pure pentacene (# 6, dotted line) and of pentacene coated nanoparticles after synthesis (# 8, solid line) and after 7 weeks of storage (# 9, dashed line). All samples are dispersed

both were in situ dispersed in ethylene glycol (Fig. 5, # 6, # 8). The absorbance spectra were corrected by subtracting the contribution of pure ZrO₂ nanoparticles in ethylene glycol (measured separately) which absorb in the region from 300 to 500 nm. Both the pentacene reference sample (# 6) and the coated

Table 2 Position of the four dominant pentacene absorption peaks and a comparison with literature

Pentacene powder, as received (sample 5) (nm)	544	584	629	673
Pentacene coated particles (sample 8) (nm)	544	583	629	667
Degraded pentacene coated particles (sample 9) (nm)	541	582	628	665
Reference data ^a (nm)	542	582	630	668

^a Kamura et al. (1974)

particles (# 8) exhibit similar spectra especially in the region between 500 and 700 nm where all peaks can be attributed to absorption in pentacene (see Table 2). The peaks observed in the wavelength range above 600 nm are characteristic for solid pentacene (Kamura et al. 1974) indicating that the pentacene is not dissolved in ethylene glycol. Two peaks at about 630 and 670 nm occur (Table 2) which are considered as fingerprint for Davydov splitting. This means that the pentacene coating exists at least partly in crystalline form which is also supported by XRD studies on consolidated powder samples showing a pronounced signature of crystalline pentacene (Sagmeister et al. 2008).

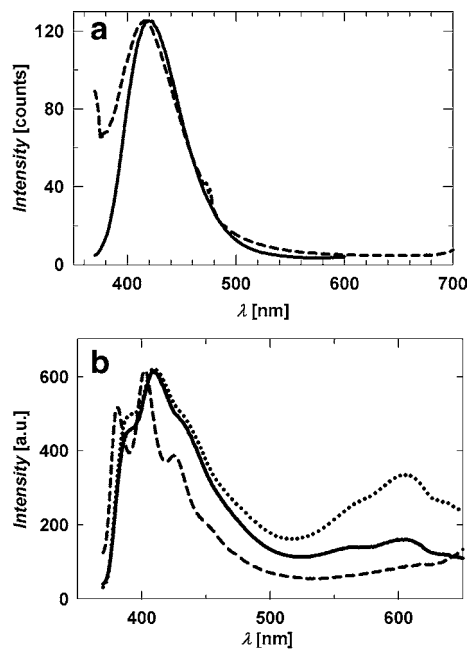


Fig. 6 PL spectra of pentacene coated ZrO_2 nanoparticles (solid line) and of pure pentacene (dashed line) as pressed pellets (**a**, samples #5, #7) and dispersed in ethylene glycol (**b**, samples #6, #8). In addition, the dispersed coated sample after 7 weeks of storage is shown (**b**, dotted line, #9)

Photoluminescence spectra were recorded on pentacene-coated ZrO_2 -nanoparticles both as powder compacts (# 7, Fig. 6a) and *in situ* dispersed (# 8, Fig. 6b). Pure pentacene was also measured as a reference (# 5, # 6). The PL spectra of pentacene-coated n- ZrO_2 (# 7, # 8) as well as those of pure pentacene (# 5, # 6) show a dominant peak at a wavelength of about 415 nm which is usually not found in pentacene. Literature data show instead for pentacene as well as for pentacene quinone (as a principal oxidized derivative) photoluminescence at wavelengths above 580 nm (Scherf and List 2002) in agreement with theoretical calculations for the energy levels in the pentacene molecule (Nijegorodov et al. 1997; He et al. 2005).

Pertaining to the origin of the dominant luminescence peak at 415 nm, it is interesting to note that a strong photoluminescence in the range of 420 nm was also reported for n- ZrO_2 and other nanoscaled oxide cores coated with polymers, such as PMMA (Vollath et al. 2004). This luminescence, which showed a blue shift with decreasing particle size, was characteristic for coated particles and considered to originate from carbonyl and ester groups at the oxide polymer interface. Therefore, the luminescence at 415 nm in the present case is tentatively attributed to oxidized pentacene derivatives. In fact, both mass spectrometry studies (see below) and data from literature indicate that pentacene may form oxidized derivatives with hydroxyl- and carbonyl functionalities (De Angelis et al., 2009). It is well known that such oxidized derivatives may act as efficient fluorescence quenchers what may explain the absence of a pentacene-specific luminescence (expected above 520 nm). On the other hand, a comparison with the absorption spectra (Fig. 5) shows that the concentration of these fluorescence quenchers is obviously below the detection limit of optical absorption.

It should be emphasized that the luminescence-active impurities were already present prior to the

synthesis process in the material as received (Fig. 5a, sample #5). In addition to these pre-existing oxide derivatives, both the optical absorption and luminescence show indication of further degradation upon storage for 7 weeks under ambient conditions (Figs. 5, 6b, sample #9). The absorption exhibits a decrease in the region from 500 to 700 nm accompanied by the appearance of new spectral features between 300 and 400 nm (# 9, Fig. 5). The latter fit quite well with spectra of pentacene quinone solutions (Itoh 1995) although it is shifted slightly, probably due to solid state effects and different solvents. Therefore, these new features and the intensity decrease of the peaks above 500 nm can be attributed to degradation of the organic material (presumably due to the formation of oxidized derivatives as pentacene quinone) during storage in air. This evidence of degradation obtained from absorption spectroscopy is further supported from the photoluminescence studies which show a significant increase in the relative PL intensity at longer wavelengths characterized by the appearance of pronounced broad peaks near 600 nm (Fig. 6b, sample #9). Again, this observation can be attributed to the formation of pentacene quinone, which in thin film exhibits photoluminescence peaks at 593 and 629 nm (Hwang et al. 2004). A degradation of the luminescent properties, demonstrated for instance by appearance of the additional emission at wavelengths above 500 nm upon prolonged exposure to air and photo-oxidation, represents a common problem of organic semiconductors (De Angelis et al. 2009; Jurchescu et al. 2004). For instance, for polyfluorenes a change of the emission color from blue to green and the formation of an emission band in the range of 2.2–2.3 eV were attributed to such keto-defects (Scherf and List 2002).

The photoluminescence spectra measured on the powder-compacted and the dispersed samples show characteristic differences (compare Fig. 6a and b). Whereas in the PL spectra of the powder samples (Fig. 6a) only a broad and featureless peak occurs, in dispersed pentacene (#6, Fig. 6b) three overlapping peaks occur and also in the pentacene-coated dispersed sample (#8, Fig. 6b) a three-peak structure can be discerned from the two shoulders of the dominant peak. This peak structure is characteristic of vibronic transitions. The presence of only one broad peak in the powder samples suggests a high degree of

interaction between the luminescent molecules in the solid state, smearing out any vibrational modes in contrast to spectra recorded on diluted dispersions. Both in the powder sample and the dispersed sample, the PL spectra of the coated particles are slightly red-shifted in comparison to pure pentacene. This observation is ascribed to an interaction of the pentacene molecules with the oxide cores and within the small agglomerates (Sagmeister et al. 2008).

For further characterization of the degradation process, the samples were also characterized by means of mass spectrometry. In addition to pentacene-coated nanoparticles, pentacene in the state as received and after purification was studied. Figure 7a shows the positive ion LDI mass spectrum obtained for pentacene powder purified twice by vacuum sublimation under a temperature gradient. Only one important species was detected. The signal at $m/z = 278.1$ is assigned to the mono-isotopic peak of the molecular ion of pentacene ($C_{22}H_{14}$).

In contrast to this, the positive ion LDI spectrum of pentacene powder ‘as-received’ showed significant additional signals at m/z values of 294.1, 295.2 etc. (Fig. 7b). The peak at mass to charge ratio of $m/z = 294.1$ is interpreted as the mono-isotopic peak of the molecular ion of single oxidized pentacene, i.e., hydroxy-pentacenes with the formula $C_{22}H_{14}O$. Note that the relative intensity observed at 295.2 is too high in comparison to the theoretical isotope pattern of $C_{22}H_{14}O$. This can be explained assuming simultaneous formation of molecular ions M^+ and pseudo-molecular ions $[M+H]^+$, a process often observed in positive LDI or MALDI spectra. In negative ion LDI mass spectra (not shown here), pentacene was observed as molecular anion at $m/z = 278.1$, while the hydroxy-pentacenes were observed as anion $[M - H]^-$ at $m/z = 293.1$. These signals were also detected in the negative ion LDI mass spectrum of coated nanoparticles (Fig. 7c). Additional signals indicating further oxidation were observed, too. For example, the signal at $m/z = 308.1$ is interpreted as the mono-isotopic peak of molecular anions of quinones with the formula $C_{22}H_{12}O_2$ (Natsume 2008).

Summarizing the mass spectrometry, indication of oxidation-products of pentacene with both hydroxy- and carbonyl-functionalities was found. It is important to note that a small fraction of oxidized pentacene already occurs in the pentacene powder as purchased. Since no data of the ionisation probabilities of the

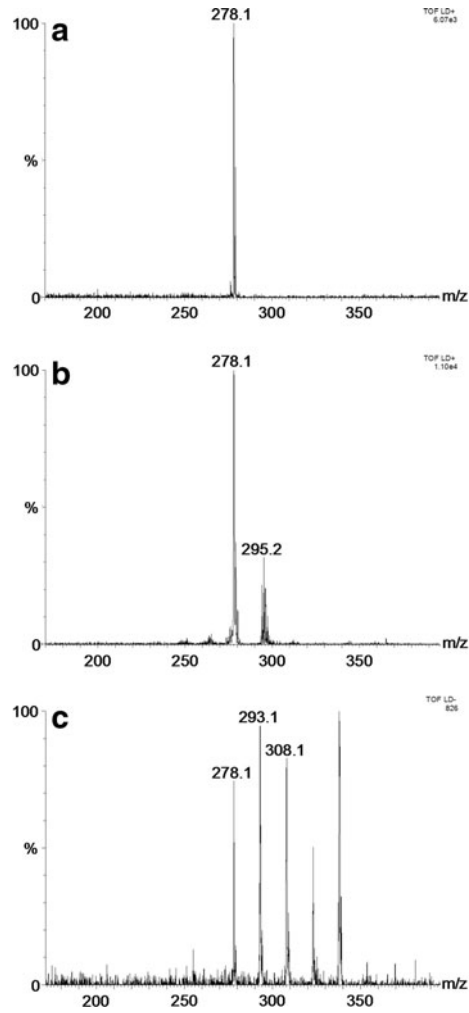


Fig. 7 Positive ion LDI mass spectra of twice purified pentacene (**a**) and as received pentacene (**b**) and negative ion LDI mass spectrum of coated nanoparticles after synthesis (**c**)

individual species are available, the mass spectra offer qualitative, but not quantitative information. A comparison of Fig. 7 with literature data shows that in case of the pentacene-coated particles, our findings of oxidized derivatives are similar to previous results for pentacene films exposed to visible light in humid air (De Angelis et al. 2009), whereas the pentacene reference powder used in our study contained mainly hydroxyl-pentacene rather than pentacene quinone (Jurchescu et al. 2004). The formation of additional oxidized pentacene derivatives (Fig. 7c) may be attributed to the presence of oxygen, water, and UV light originating from the plasma zone during synthesis.

Para-hexaphenyl-coated nanoparticles

PL spectra on ZrO_2 nanoparticles coated with para-hexaphenyl are shown in Fig. 8 along with a spectrum of a reference samples. The PL spectrum of the consolidated powder samples of p-6P-coated n- ZrO_2 (# 11) is similar to that of pure p-6P (# 10). Both are in good agreement with literature data of p-6P (Ariu et al. 1999). In the case of the suspended sample (# 12), the PL spectrum shows only one broad feature, which may be attributed to solution effects in ethylene glycol.

It is interesting to note that para-hexaphenyl shows a markedly different behavior than pentacene and anthracene. In the case of p-6P, no spectral shift for coated particles occurs in comparison to the pure coating materials in the state as received. This may be attributed to a smaller influence of the oxide cores on the energy levels of p-6P due to twisted molecule structure in comparison to the planar polyacenes. The different molecular structure may also explain that for p-6P detailed spectral features are observed for powder samples (# 10, 11), whereas dispersions show strong broadening. For pentacene, on the other hand, detailed spectral features, especially at larger wavelengths are only observed in suspensions.

Para-hexaphenyl-coated samples also showed much better air stability compared to pentacene-coated samples. Even after 6 months of storage no aging effects could be observed in the PL spectrum. That means, in contrast to pentacene, no degradation of the p-6P was observed neither due to UV radiation

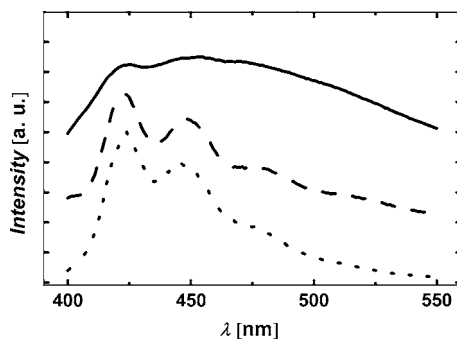


Fig. 8 PL spectra of para hexaphenyl coated ZrO_2 nanoparticles as powder sample (# 11, dashed line) and in situ dispersed in ethylene glycol (# 12, solid line) in comparison to para hexaphenyl reference powder sample (# 10, dotted line)

emitted by the plasma or thermal load during synthesis nor due to storage at ambient conditions.

Summary

Using the microwave plasma technique, oxide nanoparticles coated with a functional organic shell of anthracene, pentacene, or para-hexaphenyl were successfully synthesized. In all the cases, powders as well as dispersions have been synthesized. Transmission electron microscopy confirmed a uniform small size (~ 5 nm) of the particles. Electron energy loss and optical absorption spectroscopy gave indications for organic semiconductor coating of the ZrO_2 nanoparticles.

For all the three nanocomposite systems, photoluminescence spectra were measured on powder-compacted and in situ dispersed samples and compared with the pure coating materials. In the case of anthracene, the PL spectra of powder samples show a blue shift and increase in intensity of the main line at 408 nm and a decrease at longer wavelengths in comparison to pure anthracene. No difference was observed after dispersion in ethylene glycol. For para-hexaphenyl, no spectral shift was observed, however, dispersions of coated particles showed large peak broadening.

For pentacene, the absorption spectra of both coated nanoparticles and pentacene as received match well with literature data. The photoluminescence spectra were, however, dominated by peaks around 415 nm not reported in literature for pentacene. This behavior may be attributed to a quenching of the fluorescence by a small concentration of oxidized derivatives of pentacene with carbonyl and hydroxy groups.

In the case of anthracene and p-6P, no degradation during the synthesis and coating process or subsequent storage was observed. This shows the possibility to synthesize suitable organic/inorganic nanocomposites without altering the organic coating material. In the case of pentacene-coated n-ZrO₂, both photoluminescence and mass spectroscopy show the progressive formation of oxidized derivatives during the synthesis process and subsequent storage.

Acknowledgments Financial support by the Österreichische Forschungsförderungsgesellschaft (FFG, Project Cluster 0702

ISOTEC) is appreciated. Anja Haase, Institute of Nanostructured Materials and Photonics, Joanneum Research, Weiz, contributed purified pentacene.

References

- Ahn CC, Krivanek OL (1983) EELS Atlas. Gatan Inc, Pleasanton, CA
- Anthony JE (2007) The larger acenes: versatile organic semiconductors. *Angew Chem Int Ed* 46:452–483. doi:10.1002/anie.200604045
- Ariu M, Bongiovanni G, Loi MA, Mura A, Piaggi A, Rossi L, Graupner W, Meghdadi F, Leising G (1999) Radiative defects and optical response in oriented *para* hexaphenyl films. *Chem Phys Lett* 313:405–410. doi:10.1016/S0009-2614(99)00982-3
- Böberl M, Kovalenko MV, Gamerith S, List EJW, Heiss W (2007) Inkjet printed nanocrystal photodetectors operating up to 3 μ m wavelengths. *Adv Mater* 19:3574–3578. doi:10.1002/adma.200700111
- Brossmann U, Sagmeister M, Pölt P, Kothleitner G, Letofsky Papst I, Szabó DV, Würschum R (2007) Microwave plasma synthesis of nano crystalline YSZ. *Phys Stat Sol (RRL)* 1:107–109. doi:10.1002/pssr.200701019
- Brown AR, Pomp A, de Leeuw DM, Klaassen DBM, Havinga EE, Herwig P, Müllen K (1996) Precursor route pentacene metal insulator semiconductor field effect transistors. *J Appl Phys* 79:2136–2138. doi:10.1063/1.361071
- De Angelis F, Gaspari M, Procopio A, Cuda G, Di Fabrizio E (2009) Direct mass spectrometry investigation on pentacene thin film oxidation upon exposure to air. *Chem Phys Lett* 468:193–196. doi:10.1016/j.cplett.2008.12.048
- Dimitrakopoulos CD, Malenfant PRL (2002) Organic thin film transistors for large area electronics. *Adv Mater* 14:99–117. doi:10.1002/1521-4095(20020116)14:2<99::AID-ADMA99>3.0.CO;2-9
- Era M, Tsutsui T, Saito S (1995) Polarized electroluminescence from oriented *p* sexiphenyl vacuum deposited film. *Appl Phys Lett* 67:2436–2438. doi:10.1063/1.114599
- Gordon ML, Tulumello D, Cooper G, Hitchcock AP, Glatzel P, Mullins OC, Cramer SP, Bergmann U (2003) Inner shell excitation spectroscopy of fused ring aromatic molecules by electron energy loss and X ray Raman Techniques. *J Phys Chem A* 107:8512–8520. doi:10.1021/jp035607r
- Gundlach DJ, Jackson TN, Schlam DG, Nelson SF (1999) Solvent induced phase transition in thermally evaporated pentacene films. *Appl Phys Lett* 74:3302–3304. doi:10.1063/1.123325
- He R, Tassi NG, Blanchet GB, Pinzuk A (2005) Fundamental optical recombination in pentacene clusters and ultrathin films. *Appl Phys Lett* 87:103–107. doi:10.1063/1.2040011
- Hwang DK, Kim K, Kim JH, Im S, Jung DY, Kim E (2004) Structural and optical properties of 6, 13 pentacenequinone thin films. *Appl Phys Lett* 85:5568–5570. doi:10.1063/1.1832759
- Itoh T (1995) Low lying electronic states, spectroscopy, and photophysics of linear *para* acenequinones. *Chem Rev* 95:2351–2368. doi:10.1021/cr00039a004

- Jurchescu OD, Baas J, Palstra TTM (2004) Effect of impurities on the mobility of single crystal pentacene. *Appl Phys Lett* 84:3061–3063. doi:10.1063/1.1704874
- Kamura Y, Shirotani I, Inokuchi H (1974) Absorption spectra of oriented and amorphous naphthacene and pentacene films. *Chem Lett* 3:627–630. doi:10.1246/cl.1974.627
- Lakowicz JR (2006) Principles of fluorescence spectroscopy, 3rd edn. Springer, New York
- Lumb MD (1978) Luminescence spectroscopy. Academic Press, New York
- Minakata T, Natsume Y (2005) Direct formation of pentacene thin films by solution processing. *Synth Met* 153:1–4. doi:10.1016/j.synthmet.2005.07.210
- Natsume Y (2008) Characterization of solution processed pentacene thin film transistors. *Phys Stat Sol (a)* 205:2958–2965. doi:10.1002/pssa.200824197
- Nijegorodov N, Ramachandran R, Winkoun DP (1997) The dependence of the absorption and fluorescence parameters, the intersystem crossing and internal conversion rate constants on the number of rings in polyacene molecules. *Spectrochim Acta A* 53:1813–1824. doi:10.1016/S1386-1425(97)00071-1
- Sagmeister M, Broßmann U, List EJW, Ochs R, Szabó DV, Würschum R (2008) In situ dispersion of ZrO₂ nano particles coated with pentacene. *Phys Stat Sol (RRL)* 2:203–205. doi:10.1002/pssr.200802079
- Scherf U, List EJW (2002) Semiconducting polyfluorenes towards reliable structure property relationships. *Adv Mat* 14:477–487. doi:10.1002/1521-4095(20020404)14:7<477::AID-ADMA477>3.0.CO;2-9
- Sizmann R (1959) Herstellung von reinstem Anthracen durch azeotrope Destillation mit Äthylenglykol. *Angew Chem* 71:243–245. doi:10.1002/ange.19590710704
- Tasch S, Brandstätter C, Meghdadi Leising G, Froyer G, Athouel L (1997) Red green blue light emission from a thin film electroluminescence device based on parahexa phenyl. *Adv Mater* 9:33–36. doi:10.1002/adma.19970090105
- Vollath D (2008) Nanomaterials an introduction to synthesis, properties and application. Wiley VCH, Weinheim
- Vollath D, Szabó DV (1999) Coated nanoparticles: a new way to improved nanocomposites. *J Nanopart Res* 1:235–242. doi:10.1023/A:1010060701507
- Vollath D, Szabó DV (2006) The microwave plasma process – a versatile process to synthesise nanoparticulate materials. *J Nanopart Res* 8:417–428. doi:10.1007/s11051-005-9014-0
- Vollath D, Szabó DV, Schlabach S (2004) Oxide/polymer nanocomposites as new luminescent materials. *J Nanopart Res* 6:181–191. doi:10.1023/B:NANO.0000034624.56366.ac
- Zhu ZT, Mason JT, Dieckmann R, Malliaras GG (2002) Humidity sensors based on pentacene thin film transistors. *Appl Phys Lett* 81:4643–4645. doi:10.1063/1.1527233

Repository KITopen

Dies ist ein Postprint/begutachtetes Manuskript.

Empfohlene Zitierung:

Sagmeister, M.; Broßmann, U.; List, E. J. W.; Ochs, R.; Szabo, D. V.; Saf, R.; Grogger, W.; Tchernychova, E.; Würschum, R.

[Synthesis and optical properties of organic semiconductor: zirconia nanocomposites.](#)

2010. Journal of Nanoparticle Research, 12.

doi: [10.5445/IR/110080145](https://doi.org/10.5445/IR/110080145)

Zitierung der Originalveröffentlichung:

Sagmeister, M.; Broßmann, U.; List, E. J. W.; Ochs, R.; Szabo, D. V.; Saf, R.; Grogger, W.; Tchernychova, E.; Würschum, R.

[Synthesis and optical properties of organic semiconductor: zirconia nanocomposites.](#)

2010. Journal of Nanoparticle Research, 12, 2541–51.

doi: [10.1007/s11051-009-9823-7](https://doi.org/10.1007/s11051-009-9823-7)

Lizenzinformationen: [KITopen-Lizenz](#)